

Electronic Supporting Information

Boosting the Long-Term Stability of All-Polymer Solar Cells by Using Natural Cellulose as Interlayer

Guan-Lin Chen,^{abc} Po-Tuan Chen,^d Ching-I Huang,^{*a} Leeyih Wang,^{*abc}

^aInstitute of Polymer Science and Engineering, National Taiwan University, Taipei, 10617, Taiwan

^bCenter for Condensed Matter Sciences, National Taiwan University, Taipei, 10617, Taiwan

^cCenter of Atomic Initiative for New Materials, National Taiwan University, Taipei 10617, Taiwan

^dDepartment of Vehicle Engineering, National Taipei University of Technology, Taipei, 10608, Taiwan

*Corresponding authors Email addresses: chingih@ntu.edu.tw, leewang@ntu.edu.tw

KEYWORDS. *Cellulose, eco-friendly, stability, all-polymer solar cells, hydrogen bonding, interfacial compatibility.*

Table S1. Photovoltaic parameters of the fabricated inverted All-PSCs based on the PBDB-T:N2200 using the ZnO and ZnO/interlayers ETLs.

Parameters	V_{oc} (V)	J_{sc} (mA/cm ²)	Fill factor (%)	PCE (%)	R_{sh} (k Ω *cm ²)	R_s (Ω *cm ²)
ZnO	0.83±0.002 (0.83)	11.91±0.18 (12.10)	59.0±0.54 (59.67)	5.84±0.09 ^a (6.06) ^b	0.66±0.14 (0.81)	8.61±0.15 (8.45)
ZnO/PEI	0.84±0.004 (0.84)	12.39±0.20 (12.81)	60.87±0.27 (61.22)	6.51±0.43 ^a (6.99) ^b	0.74±0.09 (0.88)	8.17±0.06 (8.07)
ZnO/PEIE	0.84±0.001 (0.84)	13.32±0.02 (13.34)	61.74±0.60 (62.44)	6.97±0.08 ^a (7.06) ^b	0.79±0.15 (0.97)	8.13±0.14 (7.92)
ZnO/Cellulose	0.85±0.002 (0.85)	13.08±0.39 (13.90)	63.07±0.97 (64.37)	7.03±0.11 ^a (7.33) ^b	0.93±0.11 (1.17)	7.89±0.24 (7.61)

a. The average PCEs are based on 10 devices. b. Parentheses show the values from the champion devices.

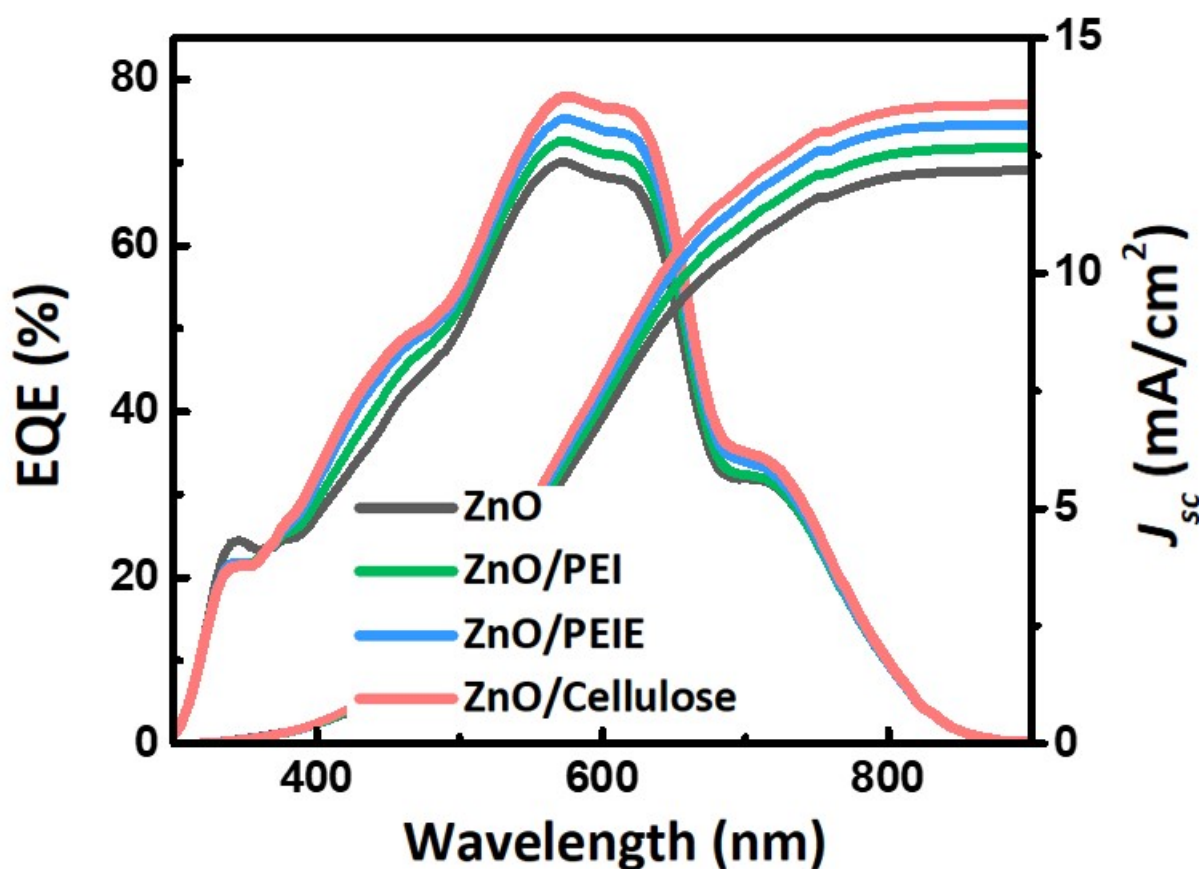


Figure S1. EQE spectra of our fabricated All-PSCs using the ZnO and ZnO/interlayers ETLs.

Table S2. The contact angle ($^{\circ}$) and surface energy data of the ZnO and ZnO/interlayers samples.¹

Compounds	ZnO	PEI	PEIE	Cellulose	PBDB-T:N2200
$\theta_{\text{water}} (^{\circ})$	40.52 ± 1.86^a	0.00^a	22.64 ± 0.58^a	51.82 ± 3.86^a	94.21
$\theta_{\text{Glycerol}} (^{\circ})$	33.66 ± 0.44^a	0.00^a	19.54 ± 1.00^a	34.89 ± 2.52^a	71.21
$\gamma_{\text{total}} (\text{N m}^{-1})$	57.33	-	67.45	52.99	40.52

a. The average contact angles are based on 5 studies interlayers.

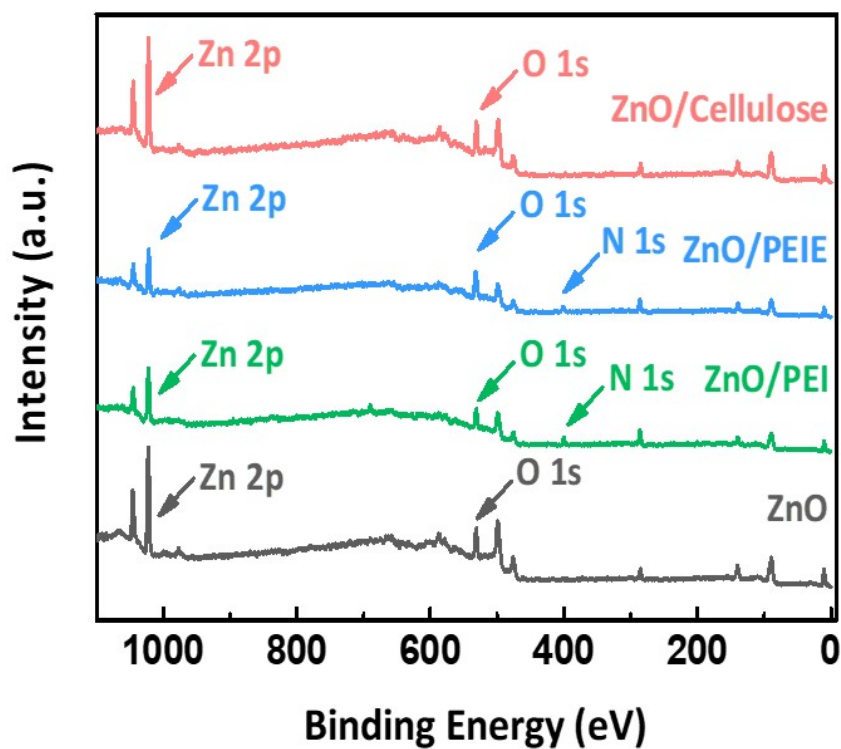


Figure S2. XPS survey spectra of the ZnO and ZnO/interlayers samples.

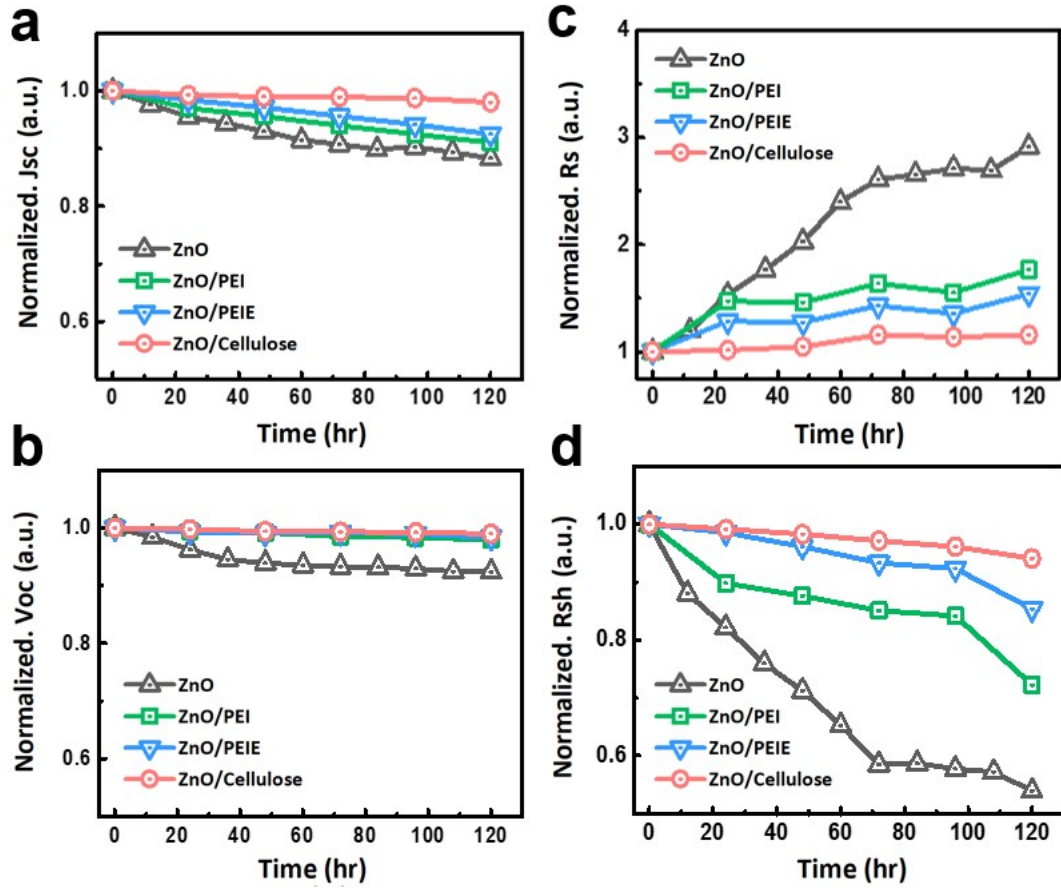


Figure S3. The evolutions of normalized (a) J_{sc} , (b) V_{oc} , (c) R_s , and (d) R_{sh} of the studied All-PSCs under the relative humidity (RH) of 40% at 25 °C.

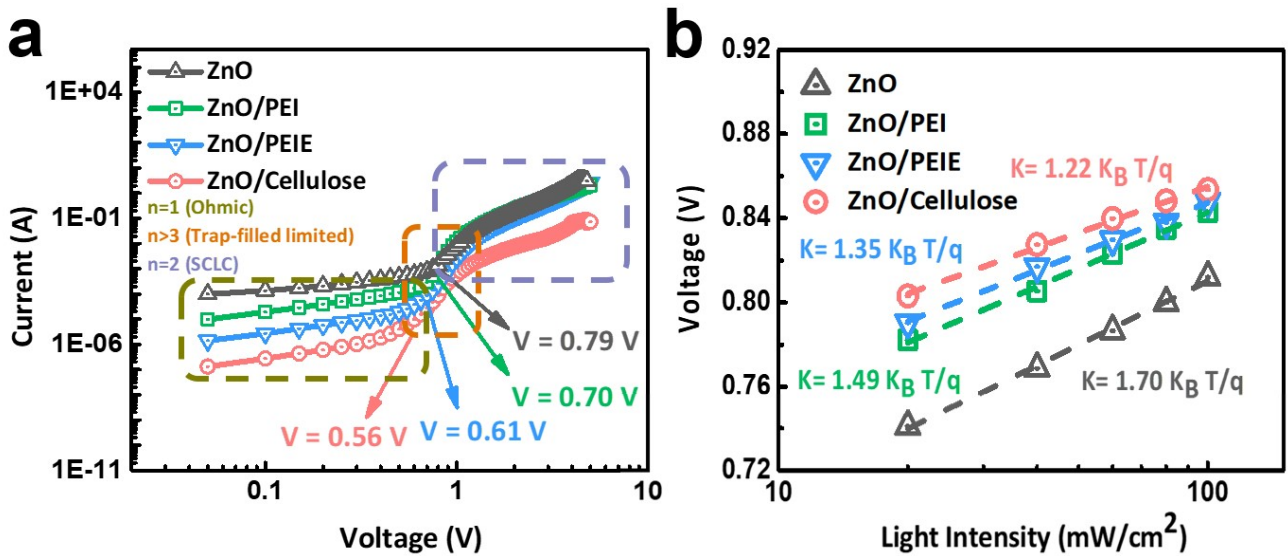


Figure S4. (a) Current-voltage traces and trap density, (b) V_{oc} versus light intensity curves.^{2,3} These devices of moisture aging are under the relative humidity (RH) of 40% at 25 °C for 48hr.

Table S3. Compared with fresh and moisture aging device with trap density, and the slope (K) of the relationship between V_{oc} and illumination intensity for ZnO and ZnO/interlayers devices.^{2,3}

Parameters	Fresh		Moisture Aging	
	N_{trap}	K ($K_B T/q$)	N_{trap}	K ($K_B T/q$)
ZnO	$2.61 \times 10^{16} \text{ cm}^{-3}$	1.34	$3.08 \times 10^{16} \text{ cm}^{-3}$	1.70
ZnO/PEI	$2.45 \times 10^{16} \text{ cm}^{-3}$	1.25	$2.73 \times 10^{16} \text{ cm}^{-3}$	1.49
ZnO/PEIE	$2.30 \times 10^{16} \text{ cm}^{-3}$	1.23	$2.38 \times 10^{16} \text{ cm}^{-3}$	1.35
ZnO/Cellulose	$2.14 \times 10^{16} \text{ cm}^{-3}$	1.21	$2.18 \times 10^{16} \text{ cm}^{-3}$	1.22

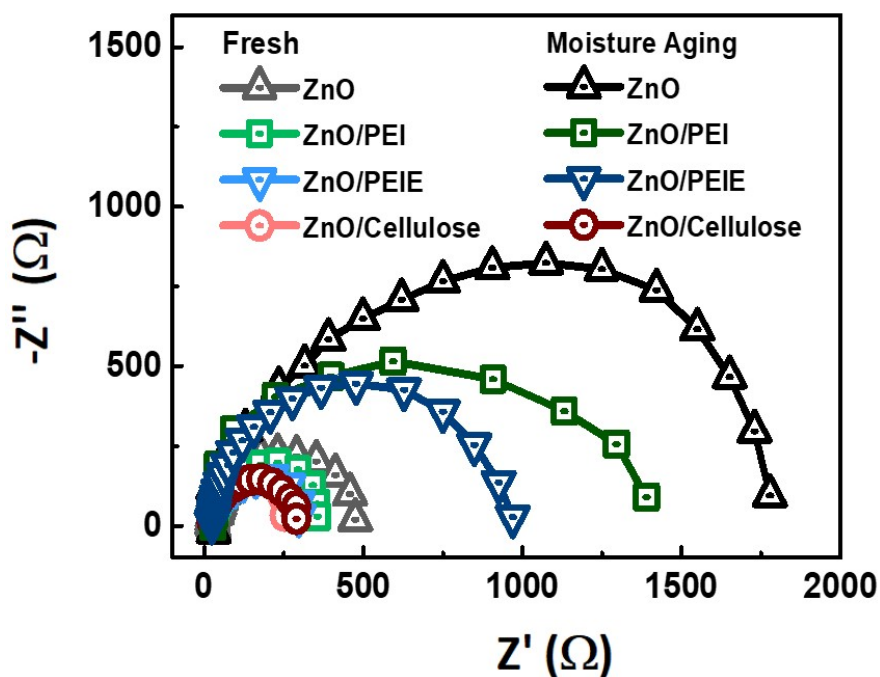


Figure S5. Nyquist plots of the All-PSCs fabricated with ZnO and ZnO/interlayers after moisture aging under 40% relative humidity (RH) at 25°C for 48 hours, compared with the plots of fresh

devices.⁴⁻⁸

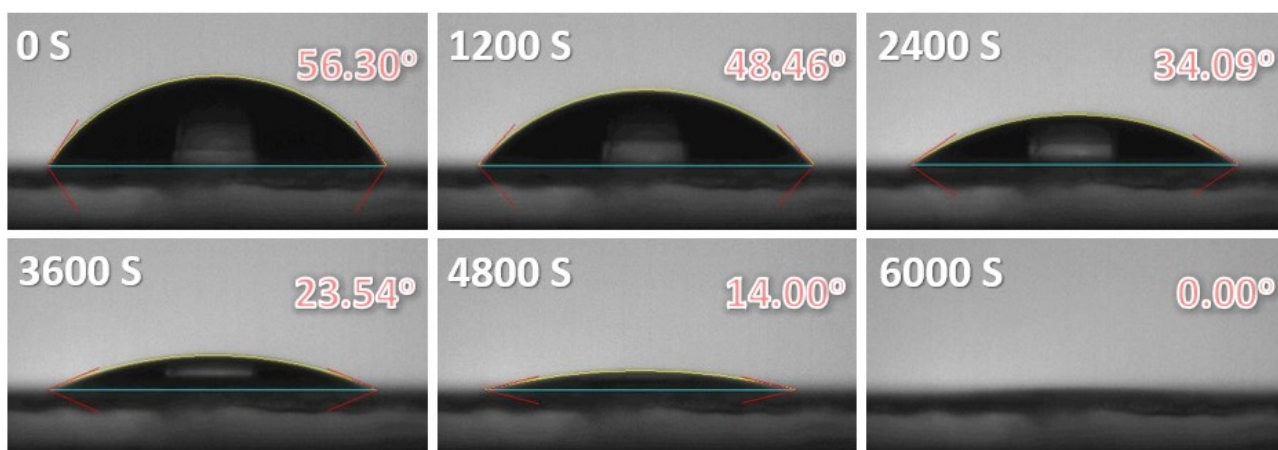


Figure S6. Variation of water droplets permeating cellulose film with time.

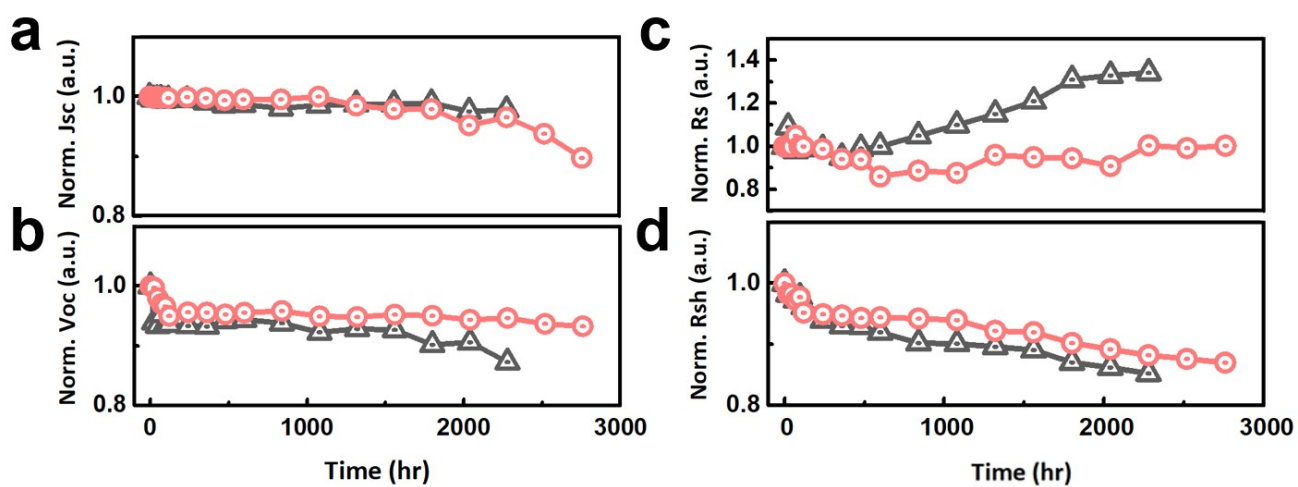


Figure S7. The evolutions of normalized (a) J_{sc} , (b) V_{oc} , (c) R_s , and (d) R_{sh} of the studied All-PSCs

under the thermal aging at 75 °C in N₂ atmosphere.

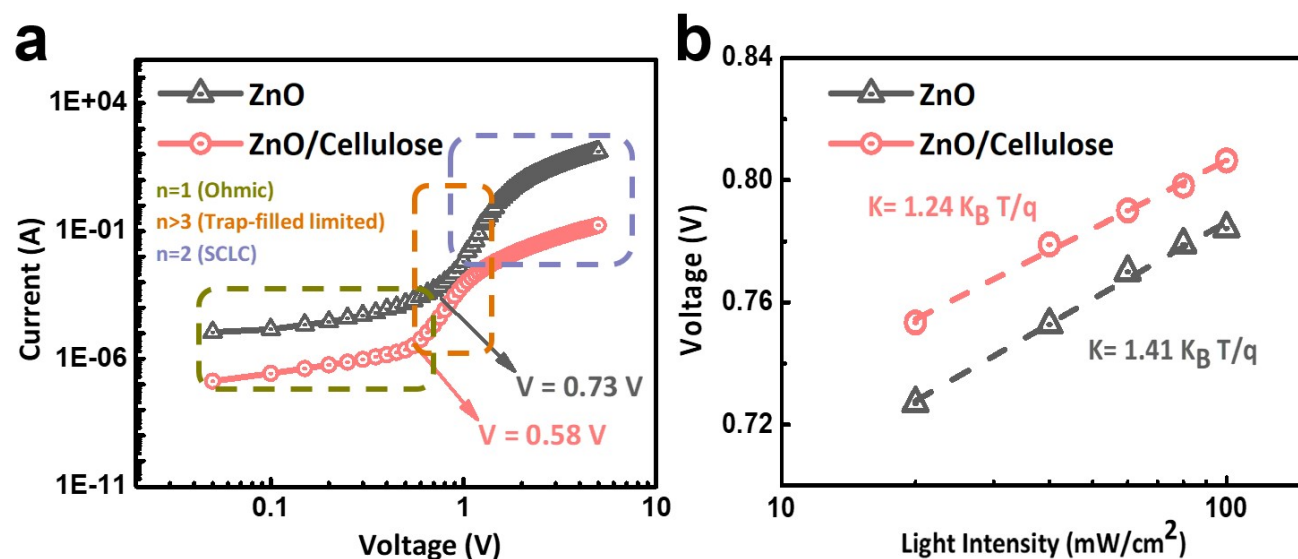


Figure S8. (a) Current-voltage traces and trap density, (b) V_{oc} versus light intensity curves.^{2, 3} These devices of thermal aging are by storing at 75 °C for 1500 hr in N₂ condition.

Table S4. Compared with fresh and thermal aging device with trap density, and the slope (K) of the relationship between V_{oc} and illumination intensity for ZnO and ZnO/interlayers devices.^{2, 3}

Parameters	Fresh		Thermal Aging	
	N_{trap}	K ($K_B T/q$)	N_{trap}	K ($K_B T/q$)
ZnO	$2.61 \cdot 10^{16} \text{ cm}^{-3}$	1.34	$2.84 \cdot 10^{16} \text{ cm}^{-3}$	1.41
ZnO/Cellulose	$2.14 \cdot 10^{16} \text{ cm}^{-3}$	1.21	$2.26 \cdot 10^{16} \text{ cm}^{-3}$	1.24

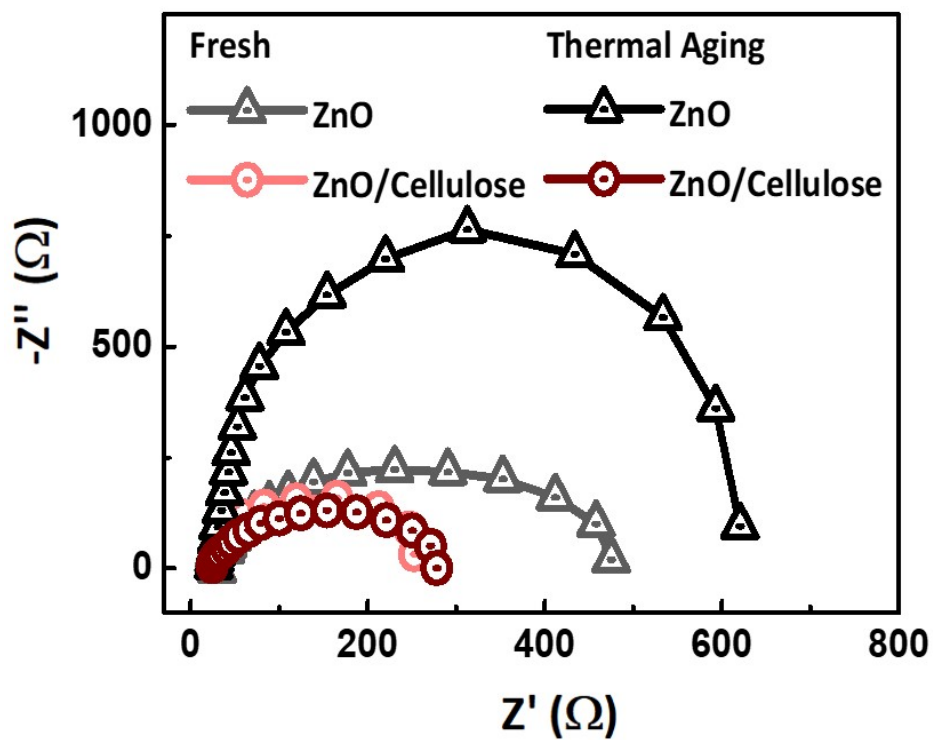


Figure S9. Nyquist plots of the All-PSCs fabricated with ZnO and ZnO/interlayers after thermal aging at 75°C for 1500 hours in N₂, compared with the plots of fresh devices.⁴⁻⁸

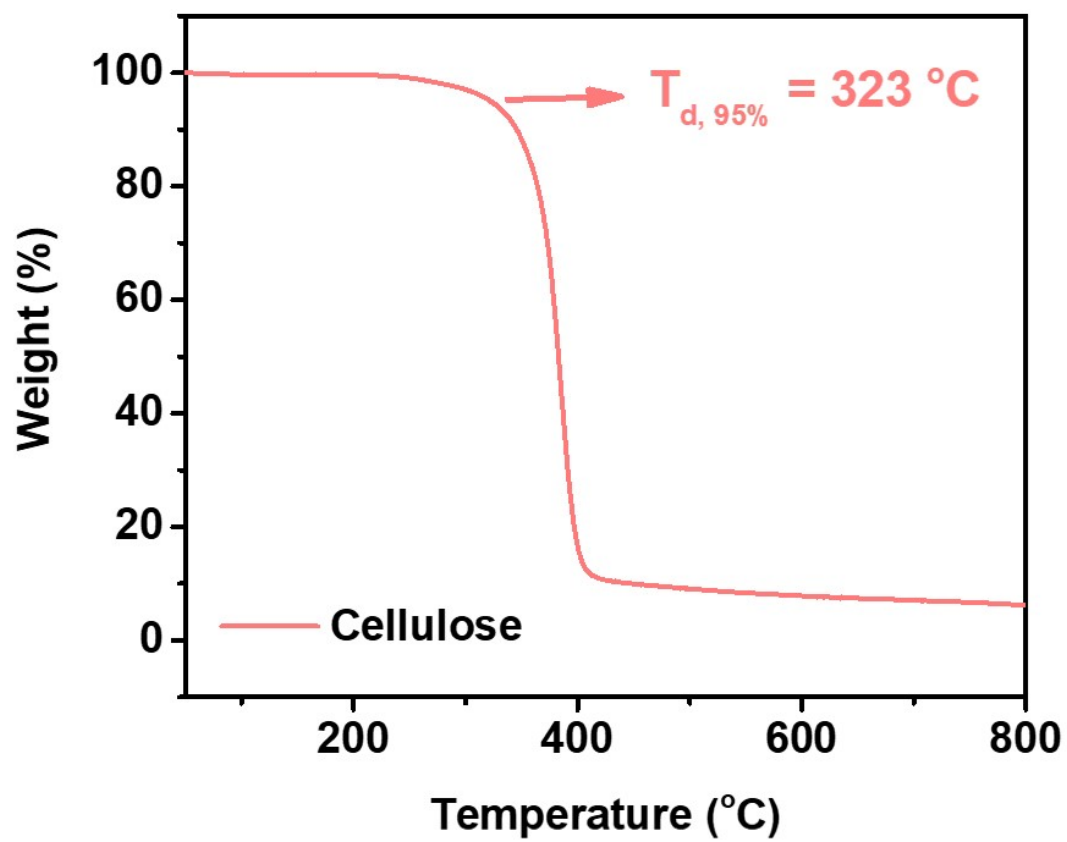


Fig. S10 TGA curve of cellulose.

Computational Models and Optimized Structure

To fundamentally investigate the interaction at the interface, first-principle calculations have been conducted through Vienna ab initial Simulation Package (VASP)⁹⁻¹¹ to evaluate the adsorption energy of PEI, PEIE, and cellulose on the ZnO surface. Herein, projector augmented wave (PAW) method is adopted and Perdew-Burke-Ernzerhof (PBE) exchange correlation functional are used to account for electron-electron interactions in our system.¹² Monkhorst-Pack K-point grids of $2 \times 2 \times 1$ and 400 eV energy cutoff for plane wave basis set are used for geometric optimization. The (0001) O-terminated surface was represented by a periodic three tri-layer (six atomic layers) slab structure in the 4×4 ZnO wurtzite supercell, where two upper tri-layers were allowed to relax while the bottom tri-layer was frozen at the bulk geometry. The geometric structures are optimized when the total energy is converged to 10^{-6} eV. The periodic cell length in z-direction (surface normal) was set at 35 Å. The vacuum layer between the adsorbed cluster and a periodic image of the slab is at least 13 Å.

Intermolecular interaction between a point defect of ZnO surface and adsorbates may play an important role at the interface. However, the calculation cost of macromolecules, such as PEI, PEIE, and cellulose, is quite expensive. Because the interface interaction is mainly attributed to the functional group $-NH_2$ of PEI, and the functional group $-OH$ of cellulose and PEIE, we truncated the macromolecule models and focused on the interface interaction via the functional groups in order to reduce computational cost. The calculation models are shown in Figure S10.

The adsorption energy (E_{ads}) is defined as the difference between the energy of the X molecule on ZnO ($X = \text{PEI}, \text{PEIE}, \text{ and cellulose model}$) and the sum of the energies of all molecules: $E_{\text{ads}} = E(X\text{-ZnO}) - [E(X) + E(\text{ZnO})]$.

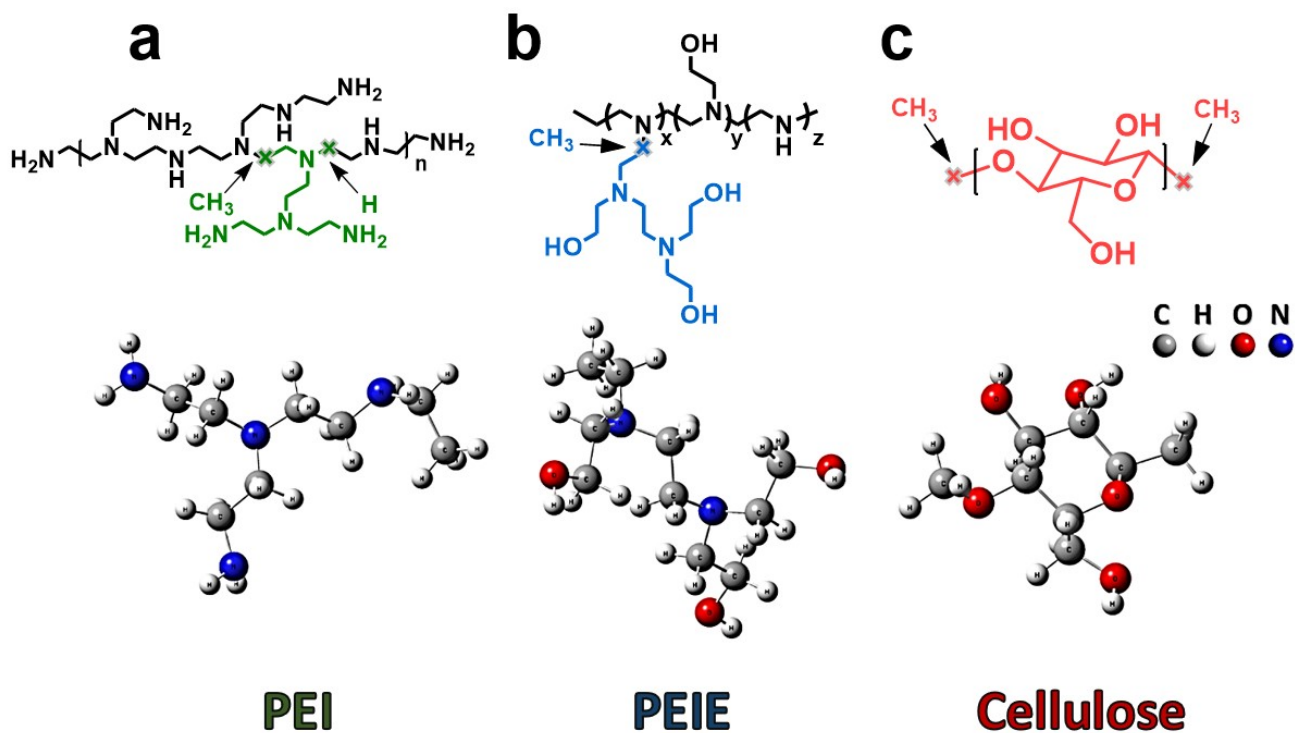


Figure S10. Calculation models of (a) PEI, (b) PEIE, and (c) cellulose molecules.

EXPERIMENTAL SECTION

Materials. PBDB-T (PCE12) and N2200 were obtained from 1-Material (Canada) and used as received. PEI, PEIE, MoO₃, chlorobenzene (CB), 2-methoxyethanol, and ethanolamine were purchased from Sigma-Aldrich without further purification. The methylcellulose (Sigma-Aldrich, Product No. M7140, CAS No. 9004-67-5) has a viscosity of 12–18 cP (2% in water at 20 °C) and a solubility of 50 mg/mL in water.

Device fabrication. Inverted All-PSCs were fabricated with a device configuration of ITO glass/ZnO or ZnO/interlayer/active layer/MoO₃/Ag. The ITO glasses underwent a thorough cleaning process, which involved sequential ultrasonic treatment in detergent, deionized water, acetone, and isopropanol, each for 30 minutes. After drying with a nitrogen flow, the substrates were subjected to 10 minutes of plasma treatment. To prepare the ZnO precursor, 100 mg of zinc acetate was dissolved in 1 mL of 2-methoxyethanol, along with 28 μ L of ethanolamine. The resulting ZnO layer was then spin-coated onto the ITO substrates at 4000 rpm for 30 seconds, followed by annealing at 220°C for 30 minutes in ambient conditions. Next, the solutions of 0.1 wt% PEI in isopropanol, 10 wt% PEIE in deionized water, and 0.1 mg/mL cellulose in deionized water were prepared. These interlayers were spin-coated onto the ZnO layer at 4000 rpm for 30 seconds and then annealed at 140°C for 10 minutes in the atmosphere. The thickness of the interlayers was estimated using a Surface Profiler (α -stepper) to be around 1 to 2 nm. For the active layer, a blend of PBDB-T:N2200 (in a 2:1 weight ratio) was

prepared by stirring the precursor solution in chlorobenzene at 65°C for 12 hours within a nitrogen glovebox. The PBDB-T:N2200 layer was then spin-coated onto the interlayers at 2000 rpm for 60 seconds, achieving an approximate thickness of 100 nm. The films were subsequently annealed at 100°C for 10 minutes inside the glovebox. Lastly, a top electrode composed of 8 nm of MoO₃ and 100 nm of Ag was thermally deposited in succession under high vacuum conditions (less than 10⁻⁶ Torr). The active area of the device measured 0.07 cm².

Characterization. The *J-V* characteristics were measured by sweeping the voltage from -0.05 to 1 V in 0.01 V increments, incorporating a delay time of 10 ms, using a Keithley 2400 source meter (Keithley Instrument Inc.). The photovoltaic performance was evaluated under one-sun intensity (100 mW cm²) using a Xenon-lamp-based solar simulator, calibrated to match the AM1.5G spectrum (EnliTech). The solar spectrum intensity was calibrated with the SRC 2020 monocrystalline silicon solar cell (EnliTech). Electrochemical impedance spectroscopy (EIS) was conducted using a Metrohm Autolab PGSTAT 320N, applying a small AC perturbation voltage of 15 mV while measuring the output current across a frequency range from 1 MHz to 1 Hz. X-ray photoelectron spectroscopy (XPS) analysis was performed with an Al-K α X-ray source ($h\nu = 1486.6$ eV) in a Theta Probe Angle-Resolved X-ray Photoelectron Spectrometer. External quantum efficiency (EQE) measurements were taken with a QE-R monochromatic light source (Enlitech Co., Ltd.), which was calibrated against a standard single-crystal silicon photovoltaic cell over a wavelength range of 300 to 800 nm. Grazing incidence wide-angle X-ray scattering (GIWAXS) measurements were conducted at beamline BL17A

at the National Synchrotron Radiation Research Center (NSRRC) in Taiwan. A cellulose film was exposed to X-rays with a wavelength of approximately 1.320 Å at a fixed incident angle of 0.2°. The resulting GIWAXS pattern was recorded using a 2D image detector (Mar345 detector). Thermogravimetric analysis (TGA) was conducted using a HITACHI STA 7200 thermogravimetric analyzer, with samples heated from 50 to 800 °C at a rate of 10 °C/min in a nitrogen environment.

Environmental stability test. For the humidity stability test, the devices underwent environmental testing in a TEN-H40 chamber (Tender Scientific Co., Ltd.), where temperature (0–100°C ± 1°C) and humidity (25–95% ± 3%) were carefully controlled. In the thermal stability test, the devices were subjected to continuous thermal stress within a nitrogen atmosphere in a glove box.

REFERENCES

1. X. Bulliard, S.-G. Ihn, S. Yun, Y. Kim, D. Choi, J.-Y. Choi, M. Kim, M. Sim, J.-H. Park, W. Choi and K. Cho, *Adv. Funct. Mater.*, 2010, **20**, 4381–4387.
2. L. Ma, S. Zhang, H. Yao, Y. Xu, J. Wang, Y. Zu and J. Hou, *ACS Appl. Mater. Interfaces*, 2020, **12**, 18777.
3. H. C. Jin, S. A. Salma, D. K. Moon and J. H. Kim, *J. Mater. Chem. A*, 2020, **8**, 4562–4569.
4. S. Huang, Y. Pang, X. Li, Y. Wang, A. Yu, Y. Tang, B. Kang, S. R. P. Silva and G. Lu, *ACS Appl. Mater. Interfaces*, 2019, **11**, 2149–2158.
5. L. Zhang, H. Zhou, Y. Xie, W. Xu, H. Tian, X. Zhao, Y. Ni, S. Y. Jeong, Y. Zou, X. Zhu, X. Ma, H. Y. Woo and F. Zhang, *Adv. Energy Mater.* **2024**, 2404718.
6. X. Chen, B. Zhu, B. Kan, K. Gao, X. Peng and Y. Cao, *J. Mater. Chem. C*, 2019, **7**, 7947–7952.
7. J. Wang, T. Chen, W. Zhao, X. Tang, Y. Bai, W. Zhou, G. Long, X. Ji, G. Lu, W. Feng, X. Wan, B. Kan and Y. Chen, *Adv. Funct. Mater.*, 2024, 2414941.
8. G.-L. Chen, S.-H. Wang, K.-W. Tseng, C.-I. Huang and L. Wang, *J. Mater. Chem. A*, 2025, **13**, 2668–2676.
9. G. Kresse and J. Hafner, *Phys. Rev. B: Condens. Matter Mater. Phys.*, 1994, **49**, 14251.
10. G. Kresse and J. Furthmüller, *Comput. Mater. Sci.*, 1996, **6**, 15–50.
11. G. Kresse and J. Furthmüller, *Phys. Rev. B: Condens. Matter Mater. Phys.*, 1996, **54**, 11169–

11186.

12. J. P. Perdew, K. Burke and M. Ernzerhof, *Phys. Rev. Lett.*, 1996, **77**, 3865–3868.